

FIGURES

Figure 1: 2°N-2°S section of ERS zonal wind stress of (a) anomalies relative to the 1993-1996 mean, (b) seasonal cycle computed over the 1993-1996 period with the 1993-1996 mean retrieved, and (c) interannual anomalies relative to the 1933-1996 seasonal cycle. Units are in N/m^2 and contour interval is 0.02 N/m^2 . Positive (negative) coefficients are white (gray).

Figure 2: Meridional structures of sea level (a) and zonal current (b) for Kelvin and first- Rossby modes (calculated for a 2m/s Kelvin phase speed). Each wave amplitude at a given latitude can be obtained by multiplying the meridional structure to the calculated coefficient, yielding to cm for TOPEX/POSEIDON sea level anomaly coefficients or N/m^2 for ERS wind stress anomaly coefficients.

Figure 3: (left) Longitude-time plots of the TOPEX/POSEIDON Kelvin wave coefficient (from 44°E to 96°E), (middle) the first-mode Rossby wave coefficient (in reverse display from 96°E to 44°E), and (right) the Kelvin wave coefficient (from 44°E to 96°E; repeated for comparison). Contour interval is 5cm for both coefficients. Positive (negative) coefficients are white (gray).

Figure 4: (a) Time series at 92°E of the Kelvin coefficient (solid line) and the first-mode Rossby coefficient lagged (backward in time) by a 10-day period corresponding to the time it takes the Kelvin wave to reach the boundary and to come back as a Rossby wave at 92°E (solid line); (b) Same as (a) but at 82°E and the first-mode Rossby coefficient is lagged by a 20-day period corresponding to the time it takes the Kelvin wave to reach the boundary and to come back as a Rossby wave at 82°E; (c) Time series at 50°E of the Kelvin coefficient (solid line), the first-mode Rossby coefficient lagged (forward in time) by a 10-day period corresponding to the time it takes the Rossby wave to reach the boundary and to come back as a Kelvin wave at 50°E (dashed line).

Figure 5: Longitude time-plot of the seasonal cycle of (a) the ERS wind coefficient integrated along the Kelvin wave characteristics (assuming a 2m/s baroclinic phase speed); (b) the reflected first-mode Rossby wave amplitude propagated along the Kelvin wave characteristics (assuming a 2m/s phase speed); (c) the TOPEX/POSEIDON Kelvin coefficient; (d) Same as (a) but along the first-mode Rossby wave characteristics; (e) the reflected Kelvin wave amplitude propagated along the first-mode Rossby wave characteristics (assuming a 2m/s baroclinic phase speed); (f) Same as (c) but for the first-mode Rossby wave. All coefficients are dimensionnalised (contour intervals are every 5cm). Anomalies are computed relative to a 4-year mean (January 1993-December 1996). Positive (negative) anomalies are white (gray)

Figure 6: Longitude time-plot of K interannual anomalies of (a) the ERS wind coefficient integrated along the Kelvin wave characteristics (assuming a 2m/s baroclinic phase speed); (b) the reflected first-mode Rossby wave amplitude propagated along the Kelvin wave characteristics (assuming a 2m/s phase speed); (c) the TOPEX/POSEIDON Kelvin coefficient. All coefficients are dimensionnalised (contour intervals are every 5cm). Interannual anomalies are computed relative to a 4-year mean seasonal cycle (January 1993-December 1996). Positive (negative) anomalies are white (gray)

Figure 7: Longitude time-plot of R1 interannual anomalies of (a) the ERS wind coefficient integrated along the first-mode Rossby wave characteristics (assuming a 2m/s baroclinic phase speed); (b) the reflected Kelvin wave amplitude propagated along the first-mode Rossby wave characteristics (assuming a 2m/s phase speed); (c) the TOPEX/POSEIDON first-mode Rossby wave coefficient. All coefficients are dimensionnalised (contour intervals are every 5cm). Interannual anomalies are computed relative to a 4-year mean seasonal cycle (January 1993-December 1996). Positive (negative) anomalies are white (gray)

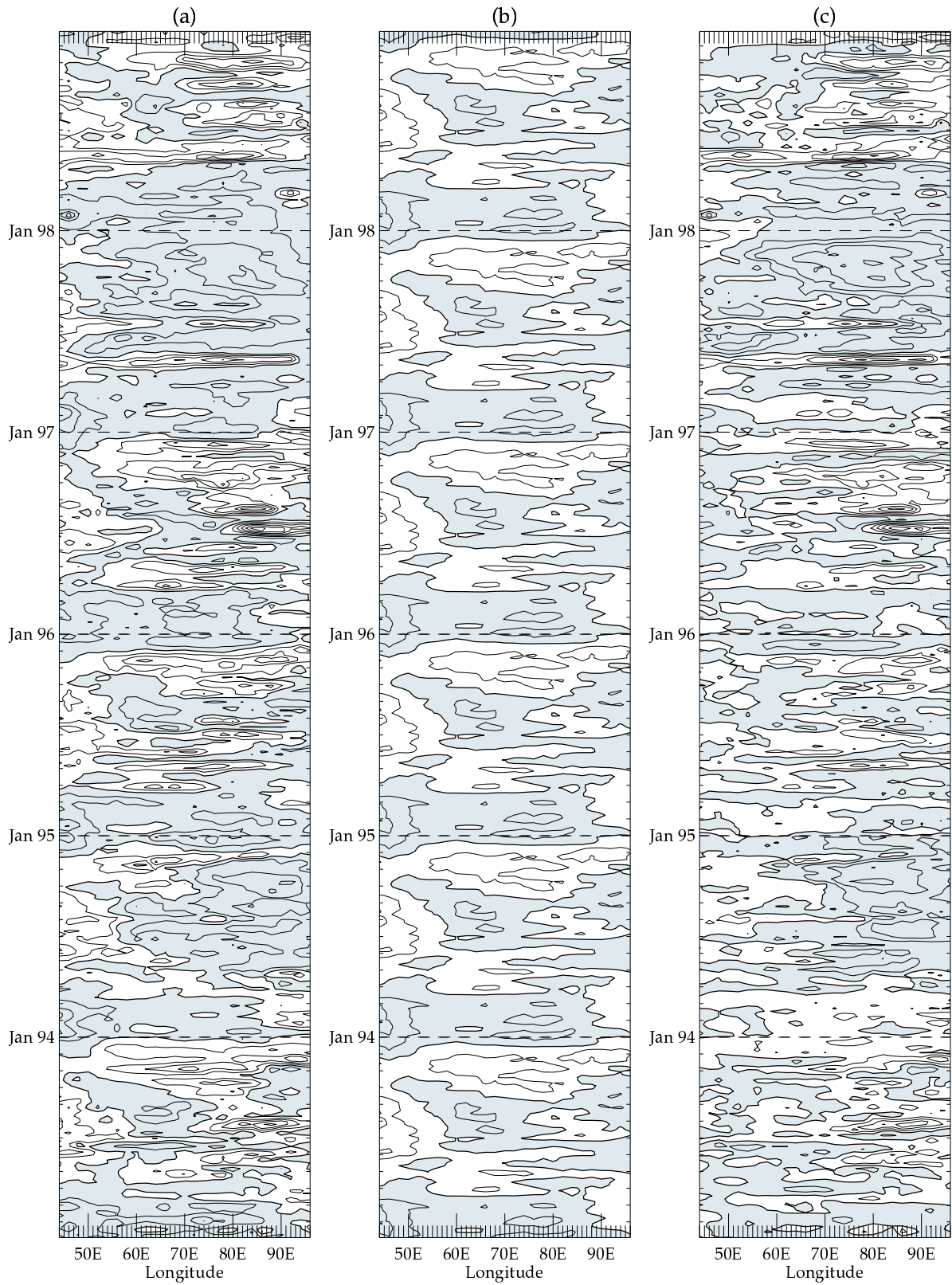


Figure 1 (Le Blanc and Boulanger, Climate Dynamics, 2000)

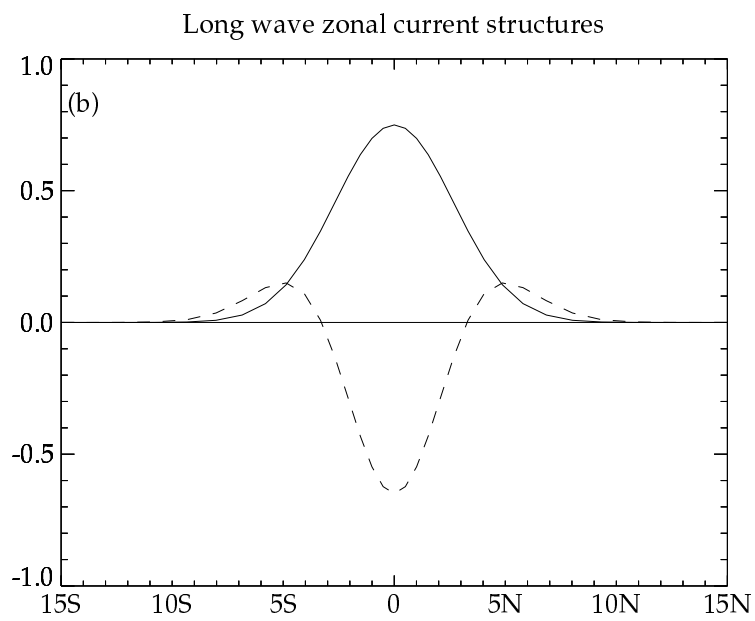
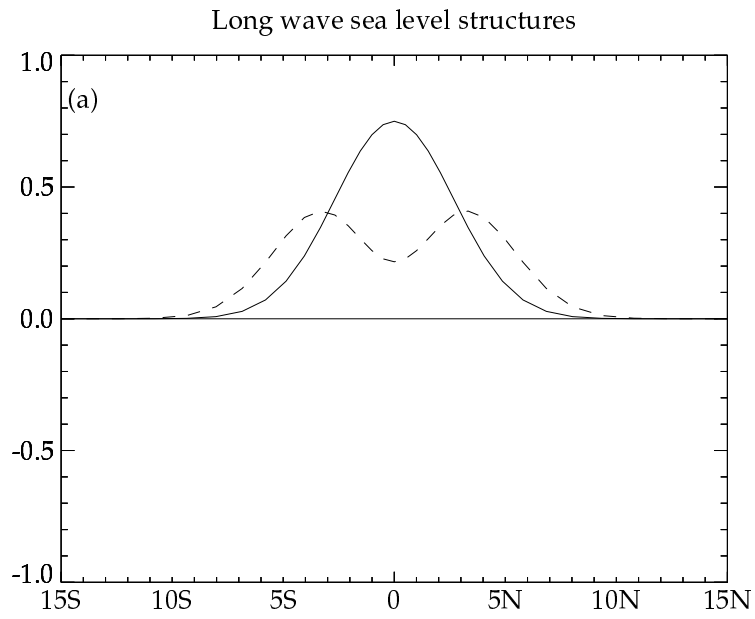


Figure 2 (Le Blanc and Boulanger, Climate Dynamics, 2000)

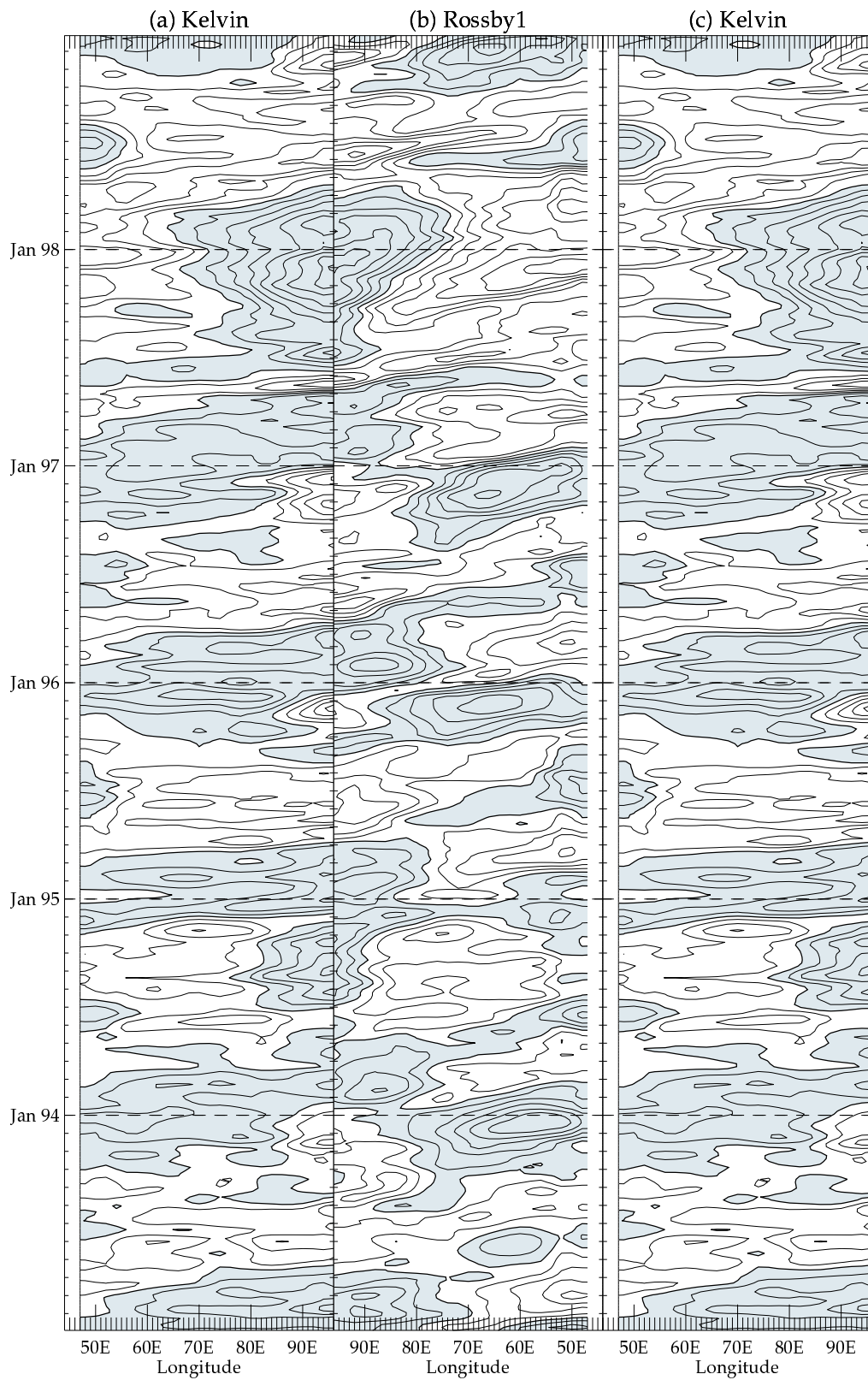


Figure 3 (Le Blanc and Boulanger, Climate Dynamics, 2000)

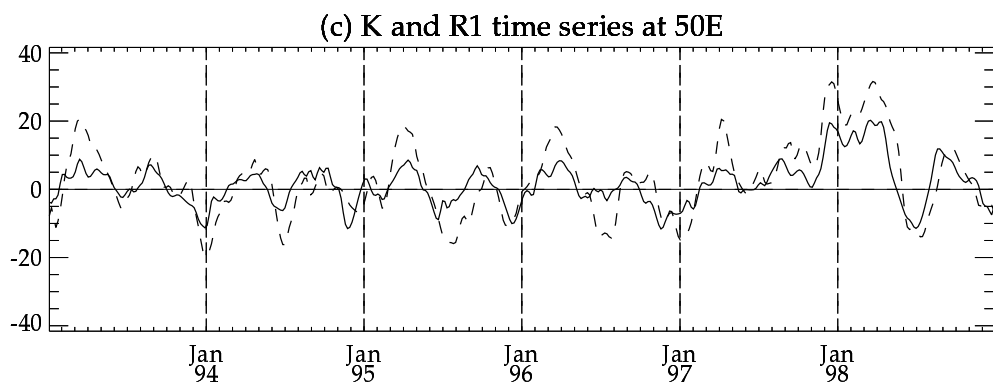
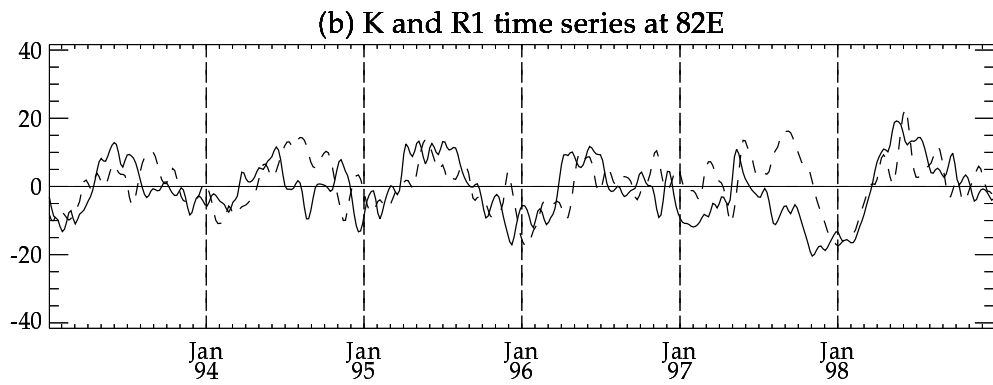
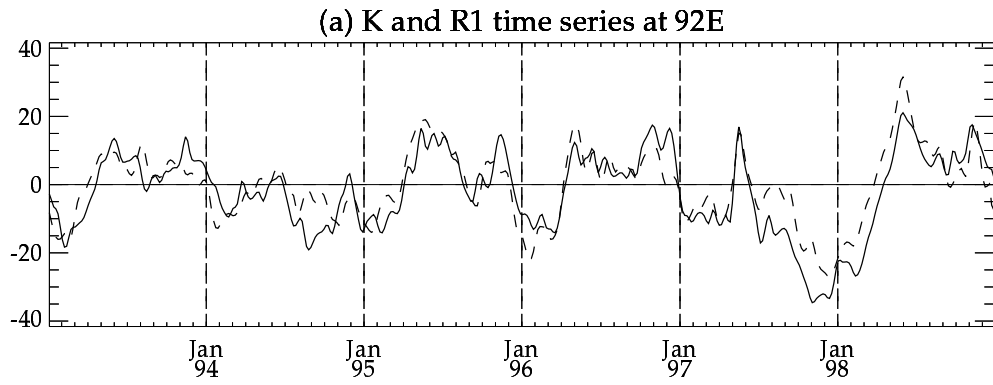


Figure 4 (Le Blanc and Boulanger, Climate Dynamics, 2000)

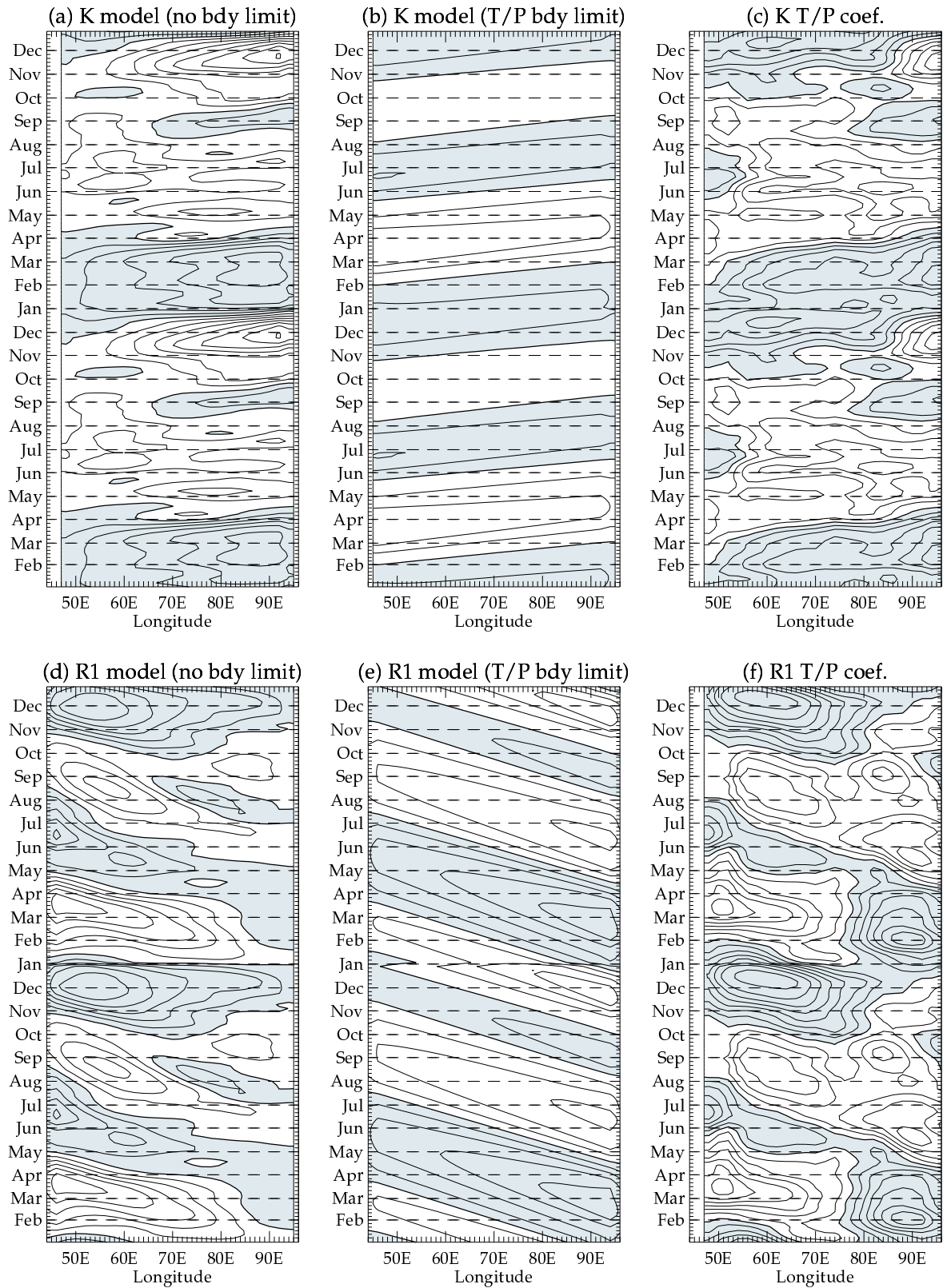


Figure 5 (Le Blanc and Boulanger, Climate Dynamics, 2000)

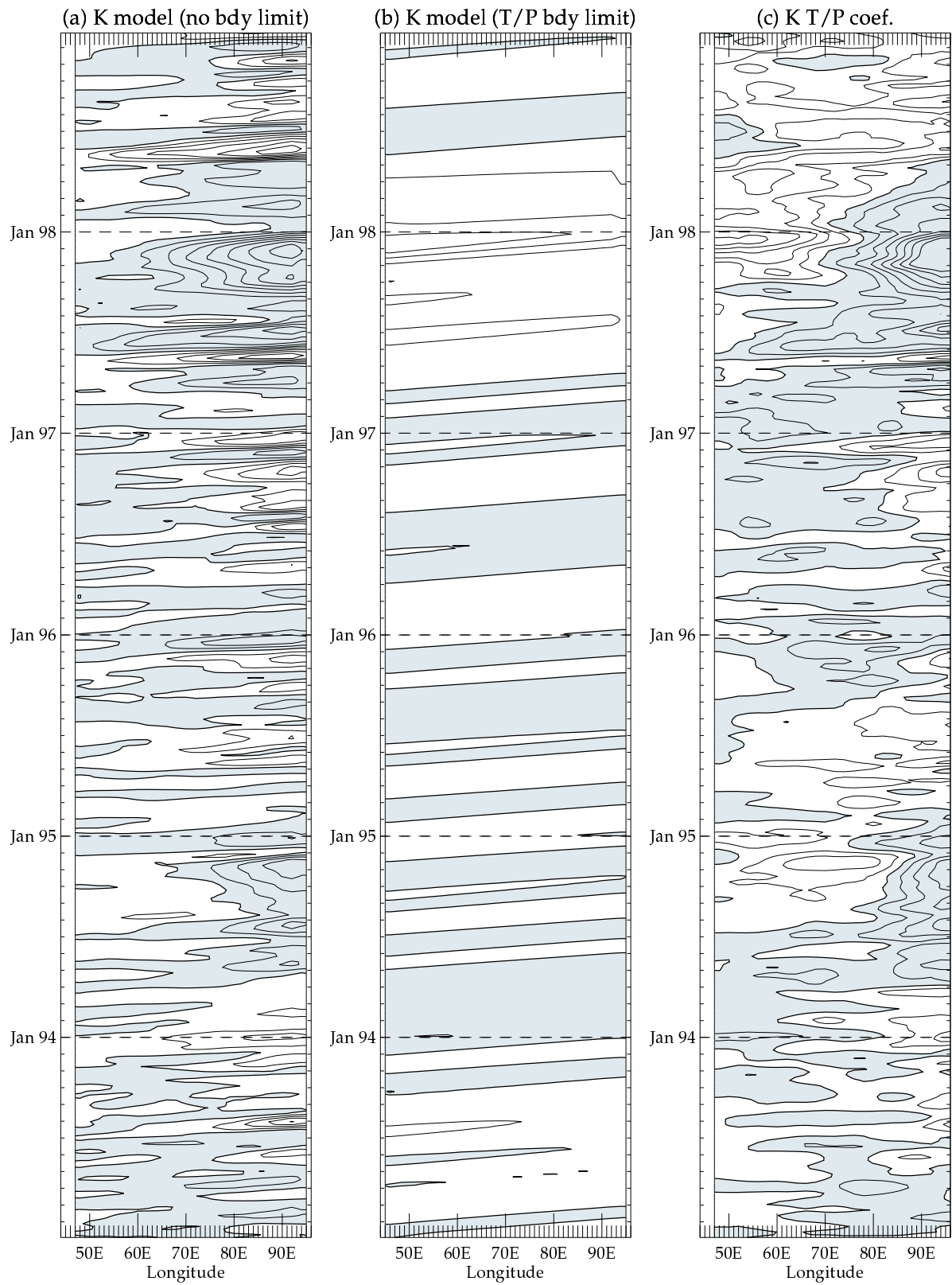


Figure 6 (Le Blanc and Boulanger, Climate Dynamics, 2000)

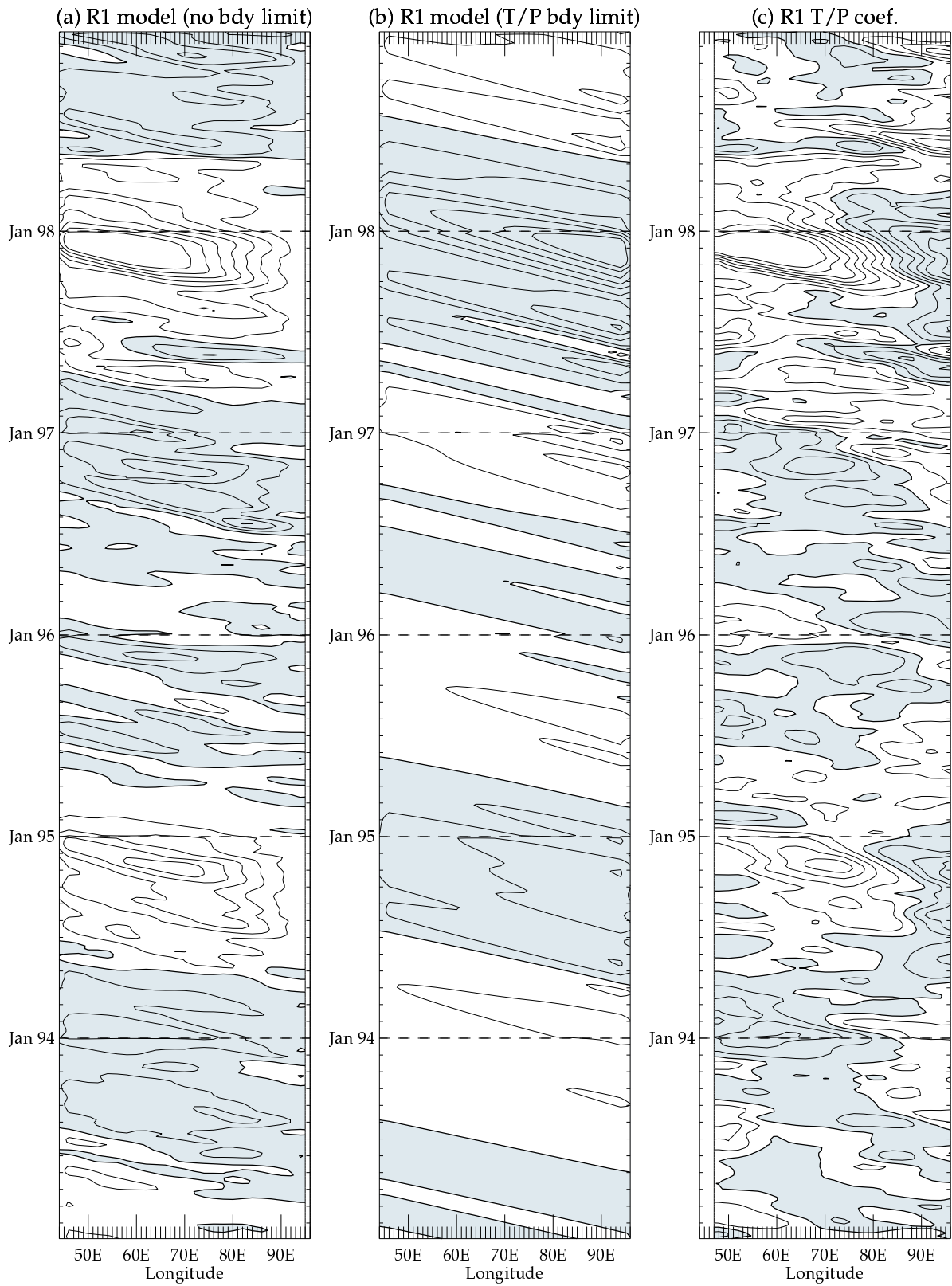


Figure 7 (Le Blanc and Boulanger, Climate Dynamics, 2000)